Proceedings of the 2025 Winter Simulation Conference
E. Azar, A. Djanatliev, A. Harper, C. Kogler, V. Ramamohan, A. Anagnostou, and S. J. E. Taylor, eds.

AGENT-BASED SIMULATION OF PRICE-DEMAND DYNAMICS IN MULTI-SERVICE CHARGING STATION

Xudong Wang[1], Yang Chen[2], Brody Skipper[1], Olufemi A. Omitaomu[2], and Xueping Li[1]

[1]Dept. of Industrial and Systems Eng., University of Tennessee - Knoxville, TN, USA
[2] Computational Sciences & Engineering Division, Oak Ridge National Laboratory, Oak Ridge, TN, USA

ABSTRACT

As the adoption of electric vehicles and hydrogen fuel-cell vehicles grows, understanding how dynamic pricing strategies influence charging and refueling behaviors becomes crucial for optimizing local energy markets. This paper proposes a simulation-based analysis of a hydrogen-electricity integrated charging station that serves both types of vehicles. A multi-agent simulation framework is developed to model the interactions between vehicles and the station, incorporating price- and delay-sensitive behaviors in decision-making. The station can dynamically adjust energy prices, while vehicles optimize their charging or refueling choices based on their utility values. A series of sensitivity analyses are conducted to evaluate how electricity pricing, infrastructure capacity, and waiting behavior impact station performance. Results highlight that moderate electricity prices maximize user participation without sacrificing profit, infrastructure should be right-sized to demand to avoid over- or underutilization, and delay-toleration also affects service outcomes, which may reach the maximum service coverage at the threshold of 45 minutes.

1 INTRODUCTION

The urgency of climate change has accelerated the global shift toward low-emission transportation. In the U.S., transportation is the largest source of greenhouse gas emissions, accounting for 27% of the total in 2023, with light-duty vehicles contributing over half (ARPA-E 2024; Congressional Budget Office 2021). As a result, Electric Vehicles (EVs) and Hydrogen Fuel-Cell Vehicles (HFCVs) have become central to the shift toward cleaner mobility systems: EVs suit short-range urban travel due to high efficiency and growing infrastructure, while HFCVs offer fast refueling and longer range, making them suitable for commercial and long-haul transport (U.S. Department of Energy 2022). Their coexistence underscores the need for diversified and scalable energy infrastructure to meet national decarbonization goals (U.S. Department of Transportation 2022).

The growing adoption of EVs and HFCVs increases pressure on refueling and recharging infrastructure (Wong et al. 2020). However, access remains limited and inconvenient for many users due to complex coordination across policymakers, manufacturers, utilities, and developers (Miele et al. 2020; Hardman et al. 2018). Traditional single-fuel stations are inadequate for mixed fleets (Staffell et al. 2019), prompting interest in multi-energy charging hubs that deliver both electricity and hydrogen (Offer et al. 2010). These hybrid stations offer flexibility and space efficiency but pose new challenges in coordinating energy flows, especially under renewable intermittency and fluctuating demand (Ursua et al. 2011).

Multi-energy stations integrate components such as solar panels, wind turbines, batteries, electrolyzers, and fuel cells to meet real-time energy needs (Lund et al. 2015). Electricity may be used for EV charging, stored, or converted into hydrogen, while hydrogen can later regenerate electricity via fuel cells (Ursua et al. 2011; Zeng and Zhang 2010). Efficiently managing these conversions requires dynamic scheduling responsive to demand and price signals (Aghaei and Alizadeh 2013). Although various optimization models address energy balancing and cost reduction, they often rely on deterministic user behavior, limiting their realism in dynamic environments.

Beyond infrastructure control, user behavior significantly affects charging station performance. Both EV and HFCV users weigh energy needs against factors like price, wait time, and convenience (Daina et al. 2017). EV users often trade off cost and delay in systems with limited capacity or dynamic pricing (Dimitropoulos et al. 2013), while HFCV users may also react to pricing and fuel availability (Manoharan et al. 2024). Behavioral models attempt to capture these decisions through utility-based and probabilistic frameworks (Zhang et al. 2011). However, many rely on simplified assumptions that may miss critical user-level dynamics.

These limitations underscore the value of simulation-based approaches for analyzing complex charging systems. While optimization offers insights under idealized assumptions, it often fails to capture emergent behaviors in uncertain settings (Bertsimas and Kallus 2020). Isolated behavioral models also overlook system-wide effects from infrastructure and renewable variability (Polemis and Spais 2020). Simulation provides a flexible alternative, enabling the study of dynamic interactions among users, energy flows, and infrastructure (Ringler et al. 2016; Kremers 2014). In particular, agent-based modeling (ABM) can represent user heterogeneity, decentralized decisions, and stochastic dynamics that are analytically intractable (Yao et al. 2023; Ringler et al. 2016).

The use of ABM has been extensively explored in energy and transportation systems for capturing decentralized, dynamic interactions. In multi-energy systems, ABM has been applied to model the coordination of electricity, heating, and mobility components (Yao et al. 2023), while in electricity markets and grids it has supported the analysis of distributed behaviors and system-level outcomes (Ringler et al. 2016). In EV-related research, ABM has been used to assess user behavior and its influence on charging infrastructure performance (Pagani et al. 2019), as well as the impact of charging strategies on energy hub management (Lin et al. 2018). However, most of these studies are limited to electricity-only infrastructure or single vehicle types. To address this gap, our work develops an agent-based simulation framework that jointly models EV and HFCV agents within a dual-energy station, incorporating behavioral responses to delay, price, and renewable variability to evaluate hybrid system performance.

In this study, we develop a detailed simulation framework for a hydrogen-electricity integrated charging station that accounts for both technical operations and user behavior. Our model incorporates delay- and price-sensitive EV and HFCV agents, real-time renewable generation, storage dynamics, and market-based electricity pricing. Through this approach, we aim to evaluate not only the station's operational performance but also the behavioral outcomes of different infrastructure and pricing strategies. The paper is organized as follows: In Section 2, we illustrate our system framework and the problem. In Section 3, we describe the simulation model with agents and actions. In Section 4, we use real-world data to do an experiment and some sensitivity analysis is produced to learn how these factors will affect this system. In Section 5, we made a summary of the paper and provide some potential future extension directions.

2 PROBLEM DESCRIPTION

This study investigates the operational and behavioral dynamics of a hybrid charging station (CS) that delivers both electricity and hydrogen services. An embedded optimization model determines energy prices based on probabilistic demand distributions. The CS integrates photovoltaic (PV) panels, wind energy, battery storage, fuel cell, hydrogen tank and grid connections to balance variable supply with fluctuating vehicle demand. While on-site solar is commonly implemented, the inclusion of wind power in our model serves an exploratory role to assess the potential benefits of diversified renewable sourcing. The wind component does not necessarily represent a turbine physically installed at the station. Instead, it can reflect a self-owned or contracted wind asset located nearby. This broader interpretation allows evaluation of localized renewable contributions beyond grid purchases, particularly in settings with limited grid flexibility. Generated electricity supports EV charging, battery storage, or hydrogen production via electrolysis. Hydrogen is stored for future HFCV refueling or converted back into electricity using fuel cells. While centralized hydrogen production currently dominates due to cost and thermodynamic efficiency, we include on-site electrolysis to examine its potential in decentralized, self-sufficient energy hubs. Hydrogen's

capacity for long-term energy storage enhances resilience against renewable intermittency. Technologies such as GenCell's GreenFSG illustrate the growing feasibility of integrating on-site hydrogen storage and ultra-efficient alkaline fuel cells into hybrid charging systems (GenCell Energy 2023).

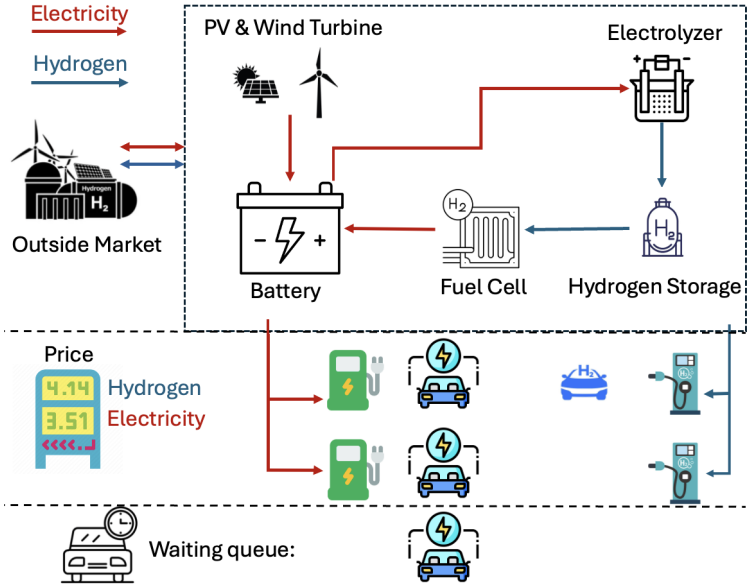

Figure 1: Energy flow in the hybrid CS.

Figure 1 illustrates the structure of the hybrid CS. The system operates under physical capacity constraints, with dedicated EV chargers and HFCV refueling stations. The CS can serve EVs and HFCVs using solar, wind, or market electricity, and can convert electricity to hydrogen via electrolysis. If stored energy is insufficient, additional electricity or hydrogen is purchased from external markets at a cost. Vehicles arrive randomly and make service decisions based on real-time energy prices and personal energy needs. A queue system handles excess demand when immediate service is unavailable.

To analyze system performance, a simulation-based framework is developed to capture interactions between renewable generation, storage, energy conversion, user behavior, and market dynamics. It evaluates how pricing strategies affect user behavior and profitability under varying conditions, offering insights for the design of future integrated multi-energy hubs.

3 SIMULATION LOGIC

In this section, we describe the simulation design using three components: agent definitions, their behavioral logic, and the operational steps executed at every time step to capture the dynamic interactions between EVs, HFCVs, and the CS.

3.1 Agent Definitions

3.1.1 EVs

Each EV agent (i) is characterized by several parameters including its battery capacity c_i, and charging speed v_i; initial state of charge (SOC) s_i, and accumulated waiting time w_i.

Figure 2 illustrates the decision-making logic of EVs. When an EV arrives at the station, it first assesses whether to enter the queue based on the queue length and its own SOC. This decision is governed by a simple balking rule: if the vehicle's SOC is above 50% and the queue length exceeds a threshold, it will leave the station; otherwise, it will join the queue. Once in the queue, the EV will wait until an electric

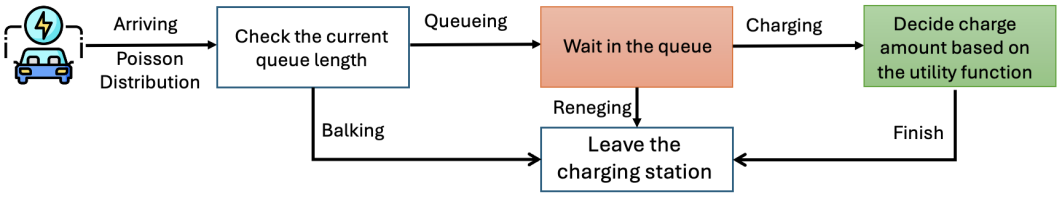

Figure 2: Decision-making logic for EV agents.

charging spot becomes available. During this period, if its waiting time w_i exceeds a threshold, the EV will renege and depart the station (Lai et al. 2022).

Upon reaching a charging spot, the EV determines how much energy to request based on its budget and utility values (Lai et al. 2023). The utility incorporates three components: (1) satisfaction from energy gain modeled as a logarithmic function, while Δt is the unit time interval of the simulation environment, α is the coefficient for perceived benefit, and Pr is the monetary value of charging utility, (2) disutility from the monetary cost of charging, while p_t is the price of electricity at time t, and (3) penalty from waiting and charging time, in which σ is the penalty for time. The utility for each time increment t is computed as:

$$U(i) = \sum_{t=1}^{T} [\alpha \cdot \log_{10}(v_i \cdot \Delta t + 1) \cdot Pr + v_i \cdot \Delta t \cdot p_t] + \sigma \cdot w_i$$

Note the summation runs from $t = 1$ to T, where T is the number of discrete time intervals in the simulation horizon (e.g., 24 hours with 5-minute intervals means $T = (60/5) * 24 = 288$ while $\Delta t = 5$). Each EV has its expected budget $B(i)$ for charging which is based on the price of electricity upon arrival at the CS, as well as its capacity and SOC. The utility value will increase when continue to charge, and it will stop charge when the utility value reaches its budget limitation, which is formulated as: $B(i) = p_t \cdot (c_i - s_i)$.

3.1.2 HFCVs

Each HFCV agent (j) possesses a fixed hydrogen tank capacity H_j, and an initial hydrogen level S_j. Figure 3 shows the decision logic of HFCVs: unlike EVs, HFCVs do not queue. To simplify the model with minimal delay sensitivity, we assume the HFCV leaves the station immediately, if all hydrogen refueling piles are occupied.

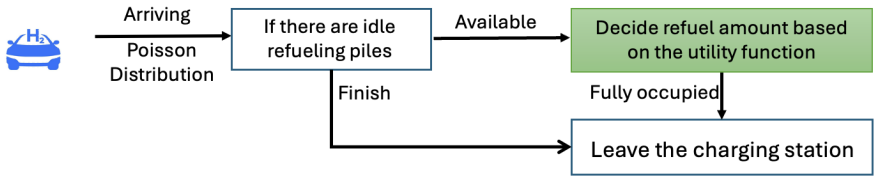

Figure 3: Behavior model of HFCV agents.

When a refueling pile is available, the HFCV computes its optimal refueling quantity h^* to maximize its utility function which equals the summation of its satisfaction value $S = \varepsilon_t \cdot H_j \cdot (1 - e^{-\beta \cdot \frac{h}{H_j}}) \cdot \frac{1}{(1-e^{-\beta})}$ (Chen et al. 2019) and refueling cost $P_t \cdot h$. The utility balances the benefit of obtaining hydrogen against the price, taking into account diminishing returns of energy. Based on Backward Induction, the closed-form solution of h^* is: $h^* = \frac{H_j}{\beta} \cdot \log\left(\frac{-\beta \cdot \varepsilon_t \cdot e^{\beta}}{P_t \cdot (1-e^{\beta})}\right)$, where β is the sensitivity to diminishing utility, ε_t is the expected value of energy utility at time t, and P_t is the price of hydrogen at time t.

3.1.3 CS

As the centralized decision-maker, the CS agent operates s_e electric charging spots and s_h hydrogen refueling piles, maintains dual storage systems for electricity and hydrogen, and manages multiple energy conversion and generation modules. Solar PV panels generate electricity based on real-time irradiance Ω_t, ambient temperature ϕ_t, transmissivity τ, panel efficiency η, degradation coefficient γ, and total surface area Area, as described in Equation 1 (Chen et al. 2023). Similarly, wind turbines produce electricity depending on wind speed V_t and turbine parameters including the rated power R_W, rated speed V_r, cut-in speed V_{ci}, and cut-out speed V_{co}, as detailed in Equation 2 (Atia and Yamada 2016).

To enable hydrogen production, the CS deploys an electrolyzer that converts surplus electricity into hydrogen, constrained by its rated capacity R_Z and minimum operational load $\underline{\alpha}_Z$. The hydrogen production depends on the electrolyzer efficiency η_Z and conversion factor κ_{ph}, shown in Equation 3. After hydrogen is produced, a compressor consumes additional electricity to store the gas in high-pressure tanks so that they can refuel HFCVs. The compression process is modeled by Equation 4 using κ_{hh} as the power consumption per unit hydrogen (Elmasry et al. 2024).

In the reverse direction, a fuel cell enables hydrogen-to-electricity conversion when needed. The output depends on the hydrogen flow rate, fuel cell efficiency η_F, conversion factor κ_{hp}, and operational bounds set by rated capacity R_H and coefficient $\underline{\alpha}_H$, as shown in Equation 5.

$$E_{\text{solar},t} = \Omega_t \cdot \tau \cdot \eta \cdot \text{Area} \cdot (1 - \gamma(\phi_t - 25)) \cdot \frac{\Delta t}{60} \quad (1)$$

$$E_{\text{wind},t} = \begin{cases} 0, & V_t < V_{ci} \text{ or } V_t > V_{co} \\ R_W \cdot \left(\dfrac{V_t^3 - V_{ci}^3}{V_r^3 - V_{ci}^3} \right) \cdot \dfrac{\Delta t}{60}, & V_{ci} \le V_t < V_r \\ R_W \cdot \dfrac{\Delta t}{60}, & V_r \le V_t \le V_{co} \end{cases} \quad (2)$$

$$hZ_t = \eta_Z \cdot pZ_t \cdot \kappa_{ph} \quad (3)$$

$$pC_t = hZ_t \cdot \kappa_{hh} \quad (4)$$

$$pF_t = \eta_F \cdot hF_t \cdot \kappa_{hp} \quad (5)$$

The CS can generate energy by itself without any costs. However, when the demand is higher that it cannot meet by itself, the CS can purchase energy from the outside market which will bring additional costs and make fewer profits.

3.2 Simulation Procedure

The simulation proceeds in discrete time intervals, emulating the real-time operation of a charging station serving both EVs and HFCVs. Each step updates the internal system state based on renewable energy generation, energy conversion, vehicle arrivals, and agent interactions.

At the beginning of each step, the CS generates electricity from solar and wind sources using real-time weather inputs and updates the energy storage levels accordingly. If energy resources are imbalanced based on the demand, the CS performs electricity-hydrogen conversion using electrolyzers and fuel cells, as described in Section 3.1.3. The prices for electricity and hydrogen are computed through an embedded optimization process that ensures budget constraints and utility maximization are satisfied based on a determined demand distribution.

New vehicle arrivals are stochastically generated based on Poisson distributions for EVs and HFCVs (Kurtz et al. 2020). Upon arrival, each EV follows the balking and reneging logic in Figure 2, joining the queue or leaving based on its state-of-charge and perceived delay. Each HFCV, governed by the model in Figure 3, refuels only if a hydrogen pile is immediately available. Charging and refueling operations are executed based on the availability of infrastructure and resource sufficiency. EVs initiate charging based on a utility-driven demand model, and HFCVs determine optimal refueling amounts analytically. Throughout

the step, profits are tracked based on energy sales and costs from external electricity and hydrogen purchases. Finally, the system updates the queue status and removes any EVs that exceed the waiting threshold. All financial and operational metrics are recorded to reflect the outcomes of each timestep.

4 EXPERIMENTS

To evaluate the dynamic performance of the CS under realistic conditions, we develop a simulation experiment using the Mesa (Project MESA 2023) framework in Python. Since we cannot simulate the real-world in continuous time, the experiment is conducted under one day with 5-minute intervals. Each agent and their actions will be considered during the whole 5-minute episode.

4.1 Primary Settings

Because this hydrogen-electricity integrated CS is currently not existing, we cannot get the actual data of them. The temperature (ϕ_t) is obtained from Weather Underground (2024), and we use National Renewable Energy Laboratory (2024) as the solar irradiation data (Ω_t) for the PV panel. And for the wind turbine, we use the historical data of wind speed (V_t) from Weather Underground (2024).

Other parameters related to the elements inside CS are the same as referred paper: the solar module adopts $\tau = 0.9$, $\eta = 0.15$, $\gamma = 0.0045$, and an area of 300 m^2; the wind turbine uses $R_W = 500$ kW, $V_{ci} = 3$ mph, $V_r = 13$ mph, and $V_{co} = 25$ mph. The electrolyzer operates with $\eta_Z = 0.6$, $\kappa_{ph} = 1/55$ kg/kWh, $R_Z = 1200$ kW, and $\alpha_Z = 0.05$. The compressor consumes $\kappa_{hh} = 2$ kWh/kg. The fuel cell uses $\eta_F = 0.65$, $\kappa_{hp} = 35$ kWh/kg, $R_H = 50$ kg/h, and $\alpha_H = 0.05$ (Chen et al. 2023; Atia and Yamada 2016; Elmasry et al. 2024).

Based on the assumption (Kurtz et al. 2020), we model the vehicle arrivals using a Poisson distribution, calibrated to reflect average hourly arrival rates of 8 EVs and 8 HFCVs, which corresponds to expected 5-minute arrival rates of $\lambda_e = \lambda_h = \frac{8}{60} \cdot 5 = 0.667$.

Each EV agent is assigned a battery capacity randomly chosen from $\{40, 80, 120\}$ kWh and a charging speed from $\{8, 10, 12\}$ kW. Initial state-of-charge values are drawn uniformly between 10% to 50% of the full capacity (U.S. Department of Energy 2025). Each HFCV agent is assigned a hydrogen tank capacity of 6 kg (TopSpeed Editorial Team 2023; BMW USA 2023; Hyfindr 2024), with a random initial hydrogen level between 1–6 kg. We do not consider large long-haul freight vehicles in the current model to make HFCVs comparable with EVs. Considering the common size of a small charge station, we set 4 electricity charging spots and 2 hydrogen refueling spots as the baseline. The CS will serve arriving EVs and HFCVs with their generated energy first, then purchase energy from the market to serve them with a lower profit. The basic price of electricity in 5-minute comes from U.S. Energy Information Administration (2024), and El-Taweel, Khani, and Farag (2018) provides an example data of hydrogen price data. Each EV has a given threshold for the maximum waiting time in the queue, which is set as 30 minutes, and all parameters for their utility function are from Table I in Lai et al. (2023).

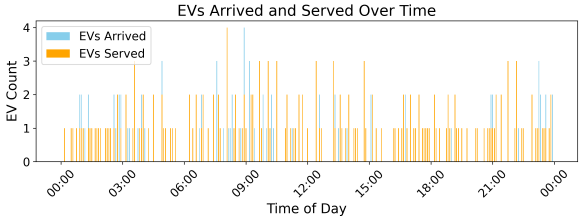

Figure 4: The number of EV arrivals and served over time.

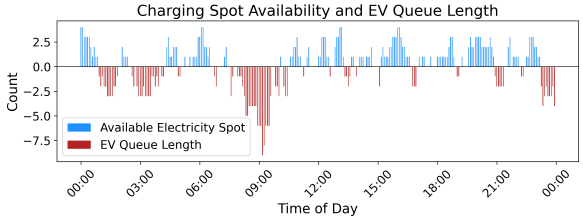

Figure 5: The number of available charging spots and EV queue length over time.

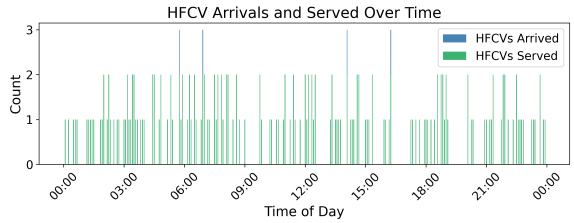

Figure 6: The number of HFCV arrivals and served over time.

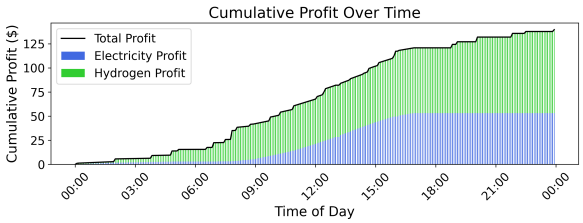

Figure 7: Cumulative profit from electricity and hydrogen.

Figure 4 shows the hourly distribution of EV arrivals and services. Due to the limitation of available electricity charging spots, there are at most 4 EVs starting charging at one time point. Comparing with Figure 6, there are more time points that both 2 hydrogen spots are fully occupied than the electricity spots. This is because EVs will take more than one time interval to get charged and make the available time of electricity spots not overlap during the time. This can also be captured from Figure 5, which shows a significant increasement on the queue length from 8 am to 10 am, which has the most EVs arriving during that time in Figure 4. Figure 7 provides a cumulative view of the CS's profit, split into electricity and hydrogen components. Notably, electricity profit dominates early and mid-day hours, while hydrogen profit contributes steadily.

4.2 Sensitivity Analysis

This section presents scenario-based sensitivity analyses to examine how key parameters affect the performance of the hybrid CS. While not aiming for global optimality, these tests compare system behavior across realistic configurations. All baseline parameters follow Section 4.1, with variations in electricity purchase price, the number of service spots, and user behavior (e.g., wait threshold, delay sensitivity). Each scenario is run over 24 hours with randomized arrivals, and results are averaged over 10 replications for robustness.

4.2.1 Behavior Changes on the Price

We investigate how fluctuations in electricity prices impact EV charging decisions and overall station dynamics. Since EVs rely on a utility function that accounts for electricity price, waiting time, and remaining power, changes in electricity prices directly affect their choice to initiate charging, balk, and renege.

To capture this behavior, we simulate multiple scenarios with adjusted electricity price ratios based on the original price, denoted as p. The station performance and EV behavioral responses are assessed under different price scaling factors ranging from $0.5p$ to $1.5p$. The results summarize key indicators such as total profit (Π), number of EVs served (N_s), number of EVs arrived (N_a), number of EVs fully charged (N_f), average waiting time (T_w), average charging duration (T_c), and total charging demand (Q). Table 1 presents a concise summary of system responses under different electricity price scenarios.

Table 1 shows the simulation results. As the electricity price rate increases from 0.5 to 1.5, the station's profit rises substantially, from \$193.91 to \$513.05. This increase indicates that, even though users reduce their charging amounts at higher prices, the elevated unit revenue offsets the lower energy consumption and maintains profitability.

However, this financial gain comes with a noticeable behavioral shift. The number of fully charged EVs declines as the price increases, falling from an average of 129.3 vehicles at a price rate of 0.5 to just 88.3 at 1.5. This suggests that EV users become more conservative with their energy demand when prices rise, likely due to the negative utility associated with high cost. Notably, even though the number of fully charged EVs declines, the total number of EVs served remains stable across all price levels, with values

Table 1: Sensitivity analysis of electricity price on station performance and EV behavior.

Price Rate	Π (\$)	N_s	N_a	N_f	T_w (min)	T_c (min)	Q (kWh)
0.5	193.91	186.6	196.9	129.3	8.55	24.72	9541.95
0.6	229.51	187.6	196.9	120.4	8.04	24.36	9464.64
0.7	257.55	187.2	196.9	113.4	7.68	23.94	9245.13
0.8	291.55	189.0	196.9	111.8	7.47	23.61	9179.87
0.9	318.12	189.2	196.9	109.8	7.29	23.45	9091.62
1.0	357.93	189.3	196.9	106.6	7.20	23.39	9094.04
1.1	395.15	189.7	196.9	102.1	6.91	23.25	9063.32
1.2	421.94	190.2	196.9	93.5	6.61	23.22	9098.17
1.3	449.41	190.6	196.9	94.1	6.59	23.08	9044.21
1.4	481.87	190.8	196.9	89.9	6.35	22.82	8941.67
1.5	513.05	191.8	196.9	88.3	6.00	22.63	8919.59

ranging between 186 and 191. This indicates that users still participate in the system but opt for shorter or partial charging sessions.

This behavior is further reflected in both the waiting and charging times. The average EV waiting time decreases from 8.55 minutes to 6.00 minutes as price increases, while the average charging duration declines from 24.72 minutes to 22.63 minutes. These trends suggest that partial charging not only shortens service time per vehicle but also improves queuing dynamics, enabling faster system turnover. Despite the decline in energy delivered—from 9541.95 kWh to 8919.59 kWh—the system maintains high throughput and user engagement, validating the effectiveness of time-sensitive pricing in managing demand without compromising service rates.

4.2.2 Optimal Spots in the CS

We investigate how different infrastructure configurations impact system performance under various vehicle arrival rates. As vehicle flow intensifies, limitations in service capacity—particularly the number of electric and hydrogen refueling spots—can lead to increased waiting time, lower service levels, and profit fluctuations. To identify these constraints and assess the effect of station scaling, we simulate multiple combinations of EV/HFCV arrival rates (λ_e, λ_h) and available charging/refueling spots (S_e, S_h).

For each configuration, we evaluate the resulting total profit (Π), number of EVs arrived (N_a), served (N_s), fully charged (N_f), average EV waiting time (T_w), average charging duration (T_c), and total EV electricity demand (Q). We also track hydrogen vehicle arrivals and service counts. There is no queueing process for HFCVs due to their fast refueling, so we have the number of HFCVs arrived (N_a^h), served (N_s^h). The results are shown in Table 2.

Table 2 explores how the CS responds to varying vehicle arrival rates and spot allocations. At low arrival rates (e.g., 4 EVs and 4 HFCVs per hour), expanding the number of electric and hydrogen spots from 2 to 8 does not significantly improve performance. In fact, the total profit slightly decreases when EV infrastructure is overbuilt under low demand scenarios. For instance, profit peaks at \$201.74 when 4 EV spots are available but drops to \$185.37 with 8 EV spots under the same arrival rate, indicating underutilization of resources.

As arrival rates increase to 6, 8, 10, and 12 vehicles per hour, infrastructure capacity becomes a critical bottleneck. When only 2 EV spots are available, high congestion leads to lower service levels. At an arrival rate of 12, the station serves just 122.1 of 282.3 EVs, with only 56.2 vehicles fully charged. In contrast, increasing EV spots to 6 or 8 significantly improves service coverage and charging outcomes. For example, with 6 EV spots, the system serves 294.4 EVs and fully charges 164.7 of them, while average waiting time drops from 25.04 minutes (2 spots) to 6.43 minutes.

Interestingly, while the number of served EVs continues to grow with more spots, profit gains begin to plateau. Maximum profitability is observed with 6 EV spots and 3 hydrogen spots, yielding \$542.71.

Table 2: Sensitivity analysis on arrival rate and service capacity configuration.

λ_e	λ_h	S_e	S_h	Π ($)	N_a	N_s	N_f	T_w (min)	T_c (min)	Q (kWh)	N_a^h	N_s^h
4	4	2	1	175.41	98.1	88.1	50.7	9.71	23.32	4194.33	102.2	86.6
4	4	4	2	201.74	98.8	98.8	66.6	0.71	24.60	5041.56	96.0	95.0
4	4	6	3	191.49	97.3	97.3	66.4	0.01	24.53	4928.69	92.8	92.7
4	4	8	4	185.37	93.8	93.8	65.6	0.00	24.86	4853.61	96.6	96.6
6	6	2	1	211.67	140.0	108.0	54.9	16.36	22.98	5081.30	148.6	116.4
6	6	4	2	279.36	146.1	144.6	90.5	2.87	24.06	7165.21	140.6	135.7
6	6	6	3	285.58	145.0	144.9	97.7	0.22	24.50	7343.77	145.0	144.0
6	6	8	4	278.42	143.1	143.1	98.2	0.01	24.46	7195.72	141.1	140.9
8	8	2	1	226.88	191.5	117.4	55.4	21.04	22.72	5474.85	187.1	136.2
8	8	4	2	357.01	198.2	190.1	109.6	7.17	23.36	9120.85	189.7	179.3
8	8	6	3	370.35	192.6	192.3	128.6	0.97	24.53	9777.10	190.5	189.3
8	8	8	4	366.42	191.6	191.6	132.2	0.05	24.81	9855.38	198.9	198.8
10	10	2	1	231.64	246.9	120.5	54.3	24.24	22.59	5607.67	239.0	162.6
10	10	4	2	398.15	229.9	211.5	113.4	10.91	23.15	10074.22	238.9	221.1
10	10	6	3	452.45	244.9	243.0	150.2	2.80	23.84	11938.76	239.3	236.1
10	10	8	4	430.73	236.4	236.3	158.4	0.39	24.33	11900.51	241.3	241.1
12	12	2	1	231.27	282.3	122.1	56.2	25.04	22.46	5622.08	288.9	179.9
12	12	4	2	432.49	283.2	232.7	113.9	16.89	22.77	10851.64	279.1	249.0
12	12	6	3	542.71	299.5	294.4	164.7	6.43	23.43	14164.09	282.2	274.6
12	12	8	4	505.52	286.1	285.5	188.7	1.09	24.24	14291.18	282.0	281.0

Expanding to 8 spots results in slightly reduced profit ($505.52), suggesting that additional capacity beyond the saturation point does not yield proportional returns and may lead to inefficiencies.

The behavior of HFCVs is comparatively less sensitive to infrastructure changes. Even with just one hydrogen refueling spot, a significant portion of vehicles are served due to short refueling times and the absence of a queue. However, adding more hydrogen spots improves the consistency and reliability of service under high arrival rates.

This experiment illustrates that infrastructure should be scaled proportionally to demand. Specifically, the rate of $\lambda_e : S_e$ should be between 1 and 2, and $\lambda_h : S_h$ should be between 0.5 and 1. While under-provisioning limits system effectiveness, over-provisioning offers diminishing returns. Identifying the optimal number of spots under different demand is key to maximizing both profit and efficiency.

4.2.3 Time Sensitivity and Waiting Behavior

In this experiment, we evaluate how EV charging behavior responds to changes in queue tolerance and delay sensitivity. Specifically, we explore two behavioral parameters: the maximum waiting time threshold (τ_w), which determines whether an EV will renege, and the time penalty factor (σ), which weighs waiting time more heavily in the utility function. These parameters reflect individual user preferences and operational policies that affect system efficiency and vehicle retention.

To analyze their effects, we simulate various combinations of τ_w ranging from 15 to 60 minutes, and σ ranging from 0.2 to 0.8. System performance is assessed using key indicators including total station profit (Π), number of EVs arrived (N_a), served (N_s), fully charged (N_f), average waiting time (T_w), charging duration (T_c), and total electricity demand (Q). Table 3 presents the results of this sensitivity analysis.

Table 3 shows that both the waiting threshold and time sensitivity significantly affect system performance. Shorter thresholds (e.g., 15 minutes) reduce average wait times but also lower profits and service rates—for example, with a time factor of 1, profit drops from $366.87 to $338.62 and EVs served from 192.7 to 173.7 as the threshold tightens. This indicates that stricter time-based balking or reneging behaviors reduce service coverage and overall revenue.

Table 3: Sensitivity analysis of wait threshold and time penalty factor on EV behavior.

τ_w (min)	σ	Π ($)	N_s	N_a	N_f	T_w (min)	T_c (min)	Q (kWh)
15	0.2	344.24	173.4	196.9	106.9	3.89	24.22	8702.48
30	0.2	366.94	188.2	196.9	109.0	7.52	23.82	9260.52
45	0.2	366.11	191.6	196.9	106.5	8.83	23.53	9259.19
60	0.2	369.63	192.4	196.9	106.3	9.96	23.55	9335.72
15	0.4	338.62	173.7	196.9	106.5	3.83	24.00	8590.29
30	0.4	357.21	189.1	196.9	108.0	6.89	23.41	9093.22
45	0.4	364.41	193.0	196.9	105.9	7.81	23.32	9264.74
60	0.4	366.87	192.7	196.9	105.0	8.83	23.50	9340.96
15	0.6	341.07	175.2	196.9	105.5	3.79	23.76	8567.55
30	0.6	361.89	189.8	196.9	104.3	7.08	23.28	9083.79
45	0.6	360.49	192.3	196.9	106.0	8.14	23.24	9200.55
60	0.6	363.51	193.1	196.9	108.7	8.07	23.21	9173.17
15	0.8	341.15	175.1	196.9	103.5	3.76	23.81	8610.78
30	0.8	358.33	189.8	196.9	102.5	7.00	23.27	9080.40
45	0.8	370.82	192.9	196.9	100.9	8.51	23.48	9389.76
60	0.8	360.07	193.3	196.9	105.5	8.25	23.11	9158.10

Higher time sensitivity (larger time factor) makes users more averse to queues, leading to shorter waits but smaller total charges. At a 15-minute threshold, increasing the time factor from 0.5 to 2 reduces profit ($344.24 to $341.15) and fully charged EVs (106.9 to 103.5), despite a similar number served. Users tend to accept shorter or partial charging sessions.

The best outcome occurs with a 45-minute threshold and time factor of 2, yielding the highest profit ($370.82) by balancing user patience and service efficiency. Although average charge duration stays around 23–24 minutes, higher time sensitivity consistently reduces energy intake. This confirms that users adapt their charging behavior not only based on electricity price but also on perceived waiting burden.

5 CONCLUSION AND FURTHER RESEARCH

This study introduces a simulation-based framework to evaluate the performance of hydrogen-electricity integrated CS under dynamic conditions. By modeling EV and HFCV interactions with real-time pricing and queues, it captures user-infrastructure dynamics. Results show that electricity pricing strongly affects user behavior—higher prices reduce per-session demand but increase profit. Infrastructure sizing also matters: both over- and under-capacity lead to inefficiencies. User behavior parameters like wait thresholds and delay sensitivity significantly influence throughput and revenue.

The proposed framework offers practical insights for sustainable infrastructure planning and CS operations. Future extensions may include stochastic renewable supply, multi-day simulations, grid trading, and policy-driven cost-benefit analysis. Reinforcement learning could also be applied for adaptive pricing and dispatch strategies. A key limitation is the simplified user behavior modeling: EVs follow deterministic balking/reneging rules, and HFCVs make binary decisions without queuing. User heterogeneity is limited to technical specs. Future work will incorporate probabilistic decisions, diverse utility functions, and learning-based behaviors to better reflect real-world dynamics.

ACKNOWLEDGMENTS

Funding: This work was supported in part by the U.S. Department of Energy's Advanced Research Projects Agency-Energy (ARPA-E) under the project (#DE-AR0001780) titled "A Cognitive Freight Transportation Digital Twin for Resiliency and Emission Control Through Optimizing Intermodal Logistics" (RECOIL).

REFERENCES

Aghaei, J., and M.-I. Alizadeh. 2013. "Demand Response in Smart Electricity Grids Equipped With Renewable Energy Sources: A Review". *Renewable and Sustainable Energy Reviews* 18:64–72.

ARPA-E 2024. "Intermodal Freight". https://arpa-e.energy.gov/technologies/exploratory-topics/intermodal-freight. Accessed: 15th October 2024.

Atia, R., and N. Yamada. 2016. "Sizing and Analysis of Renewable Energy and Battery Systems in Residential Microgrids". *IEEE Transactions on Smart Grid* 7(3):1204–1213 https://doi.org/10.1109/TSG.2016.2519541.

Bertsimas, D., and N. Kallus. 2020. "From Predictive to Prescriptive Analytics". *Management Science* 66(3):1025–1044.

Chen, Y., J. Chen, C. Liu, G. Liu, M. Ferrari, and A. Sundararajan. 2023. "Integrated Modeling and Optimal Operation of Multi-Energy System for Coastal Community". In *2023 IEEE International Conference on Electro Information Technology (eIT)*, 211–216.

Chen, Y., M. Olama, T. Rajpurohit, J. Dong, and Y. Xue. 2019. "Game-Theoretic Approach for Electricity Pricing between Distribution System Operator and Load Aggregators". In *2019 3rd International Conference on Smart Grid and Smart Cities (ICSGSC)*, 176–181 https://doi.org/10.1109/ICSGSC.2019.00005.

Congressional Budget Office 2021. "Emissions of Carbon Dioxide from U.S. Transportation in 2021". https://www.cbo.gov/publication/58861. Accessed: 5th November 2024.

Daina, N., A. Sivakumar, and J. W. Polak. 2017. "Electric Vehicle Charging Choices: Modelling and Implications for Smart Charging Services". *Transportation Research Part C: Emerging Technologies* 81:36–56.

Dimitropoulos, A., P. Rietveld, and J. N. Van Ommeren. 2013. "Consumer Valuation of Changes in Driving Range: A Meta-Analysis". *Transportation Research Part A: Policy and Practice* 55:27–45.

El-Taweel, N. A., H. Khani, and H. E. Farag. 2018. "Hydrogen Storage Optimal Scheduling for Fuel Supply and Capacity-Based Demand Response Program Under Dynamic Hydrogen Pricing". *IEEE Transactions on Smart Grid* 10(4):4531–4542.

Elmasry, Y., I. B. Mansir, Z. Abubakar, A. Ali, S. Aliyu, and K. Almamun. 2024. "Electricity-Hydrogen Nexus Integrated With Multi-Level Hydrogen Storage, Solar PV Site, and Electric-Fuelcell Car Charging Stations". *International Journal of Hydrogen Energy* 76:160–171.

GenCell Energy 2023. "GenCell Hydrogen-Based Backup Power Technology". https://www.gencellenergy.com/technology/. Accessed: 12th June 2025.

Hardman, S., A. Jenn, G. Tal, J. Axsen, G. Beard, N. Daina, *et al*. 2018. "A Review of Consumer Preferences of and Interactions With Electric Vehicle Charging Infrastructure". *Transportation Research Part D: Transport and Environment* 62:508–523.

Hyfindr 2024. "Hydrogen Tank Sizes – Overview and Applications". https://hyfindr.com/en/hydrogen-knowledge/hydrogen-tank. Accessed: 12th June 2025.

Kremers, E. A. 2014. *Modelling and Simulation of Electrical Energy Systems Through a Complex Systems Approach Using Agent-Based Models*. KIT Scientific Publishing.

Kurtz, J., T. Bradley, E. Winkler, and C. Gearhart. 2020. "Predicting Demand for Hydrogen Station Fueling". *International Journal of Hydrogen Energy* 45(56):32298–32310.

Lai, S., J. Qiu, Y. Tao, X. Sun, and J. Zhao. 2023. "Charging/Refueling Navigation Strategies for Plug-in Hybrid Hydrogen and Electric Vehicles With Irrationalities and Energy Substitution". *IEEE Transactions on Industrial Informatics* 20(1):583–595.

Lai, S., J. Qiu, Y. Tao, and J. Zhao. 2022. "Pricing for Electric Vehicle Charging Stations Based on the Responsiveness of Demand". *IEEE Transactions on Smart Grid* 14(1):530–544.

Lin, H., Y. Liu, Q. Sun, R. Xiong, H. Li, and R. Wennersten. 2018. "The Impact of Electric Vehicle Penetration and Charging Patterns on the Management of Energy Hub–a Multi-Agent System Simulation". *Applied Energy* 230:189–206.

Lund, P. D., J. Lindgren, J. Mikkola, and J. Salpakari. 2015. "Review of Energy System Flexibility Measures to Enable High Levels of Variable Renewable Electricity". *Renewable and Sustainable Energy Reviews* 45:785–807.

Manoharan, P., J. Vishnupriyan *et al*. 2024. "Designing a Comprehensive Charging Infrastructure for Environmentally Friendly Transportation: A Proposal for Evaluating Viability and Uncertainty Modeling". *Energy Conversion and Management* 322:119185.

Miele, A., J. Axsen, M. Wolinetz, E. Maine, and Z. Long. 2020. "The Role of Charging and Refuelling Infrastructure in Supporting Zero-Emission Vehicle Sales". *Transportation Research Part D: Transport and Environment* 81:102275.

National Renewable Energy Laboratory 2024. "NSRDB: National Solar Radiation Database". https://nsrdb.nrel.gov/. Accessed: 12th June 2025.

Offer, G. J., D. Howey, M. Contestabile, R. Clague, and N. Brandon. 2010. "Comparative Analysis of Battery Electric, Hydrogen Fuel Cell and Hybrid Vehicles in a Future Sustainable Road Transport System". *Energy Policy* 38(1):24–29.

Pagani, M., W. Korosec, N. Chokani, and R. S. Abhari. 2019. "User Behaviour and Electric Vehicle Charging Infrastructure: An Agent-Based Model Assessment". *Applied Energy* 254:113680.

Polemis, M. L., and A. Spais. 2020. "Disentangling the Drivers of Renewable Energy Investments: The Role of Behavioral Factors". *Business Strategy and the Environment* 29(6):2170–2180.

Project MESA 2023. "MESA: Agent-based Modeling in Python 3+". https://mesa.readthedocs.io/latest/. Accessed: 9th April 2025.

Ringler, P., D. Keles, and W. Fichtner. 2016. "Agent-Based Modelling and Simulation of Smart Electricity Grids and Markets–A Literature Review". *Renewable and Sustainable Energy Reviews* 57:205–215.

Staffell, I., D. Scamman, A. V. Abad, P. Balcombe, P. E. Dodds, P. Ekins, *et al*. 2019. "The Role of Hydrogen and Fuel Cells in the Global Energy System". *Energy & Environmental Science* 12(2):463–491.

TopSpeed Editorial Team 2023. "Hyundai Nexo HFCV Fast Facts". https://www.topspeed.com/hyundai-nexo-hfcv-fast-facts/. Accessed: 12th June 2025.

Ursua, A., L. M. Gandia, and P. Sanchis. 2011. "Hydrogen Production From Water Electrolysis: Current Status and Future Trends". *Proceedings of the IEEE* 100(2):410–426.

U.S. Department of Energy 2022. "The Role of Hydrogen Fuel Cells in Decarbonizing Transportation". https://www.energy.gov/eere/fuelcells. Accessed: 5th November 2024.

U.S. Department of Energy 2025. "Electric Vehicle Charging Station Locations". https://afdc.energy.gov/fuels/electricity-stations. Accessed: 9th April 2025.

U.S. Department of Transportation 2022. "Climate Action at DOT: Climate and Sustainability". https://www.transportation.gov/priorities/climate-and-sustainability/climate-action. Accessed: 5th November 2024.

U.S. Energy Information Administration 2024. "CAISO Wholesale Electricity Market Data". https://www.eia.gov/electricity/wholesalemarkets/data.php?rto=caiso. Accessed: 7th April 2025.

BMW USA 2023. "BMW iX5 Hydrogen". https://www.bmwusa.com/ix5-hydrogen.html. Accessed: 12th June 2025.

Weather Underground 2024. "Local Weather Forecast, News and Conditions". https://www.wunderground.com/. Accessed: 12th June 2025.

Wong, E. Y. C., D. C. K. Ho, S. So, C.-W. Tsang, and E. M. H. Chan. 2020. "Comparative Analysis on Carbon Footprint of Hydrogen Fuel Cell and Battery Electric Vehicles Based on the Greet Model". In *2020 International Conference on Decision Aid Sciences and Application (DASA)*, 932–937.

Yao, R., Y. Hu, and L. Varga. 2023. "Applications of Agent-Based Methods in Multi-Energy Systems—A Systematic Literature Review". *Energies* 16(5):2456.

Zeng, K., and D. Zhang. 2010. "Recent Progress in Alkaline Water Electrolysis for Hydrogen Production and Applications". *Progress in Energy and Combustion Science* 36(3):307–326.

Zhang, T., S. Gensler, and R. Garcia. 2011. "A Study of the Diffusion of Alternative Fuel Vehicles: An Agent-Based Modeling Approach". *Journal of Product Innovation Management* 28(2):152–168.

AUTHOR BIOGRAPHIES

XUDONG WANG is a Graduate Assistant Researcher in the Department of Industrial Systems Engineering at the University of Tennessee, Knoxville. He holds Bachelors in Information Management and Information Systems. His research interests include vehicle routing problems and simulation. His email address is xwang97@vols.utk.edu.

YANG CHEN is a Research Scientist in the Computational Urban Sciences Group within Computational Sciences and Engineering Division at Oak Ridge National Laboratory. His research interests include machine learning, optimization and simulation, with applications in power grid, urban infrastructure, and healthcare. His email address is cheny4@ornl.gov.

BRODY SKIPPER is an undergraduate student in the Department of Industrial and Systems Engineering at the University of Tennessee, Knoxville. He is pursuing his Bachelor's degree in Industrial Engineering with a minor in Engineering Management. His research interests include simulation and optimization. His email address is sdj611@vols.utk.edu.

OLUFEMI A. OMITAOMU is a Distinguished R&D Staff and Group Leader in Computational Urban Sciences group at Oak Ridge National Laboratory. His research expertise includes disaster risk analysis and urban systems resilience, energy infrastructure siting and analysis, artificial intelligence in critical infrastructure systems, and anomaly detection in complex system. He received his Ph.D. in Industrial Engineering from the University of Tennessee, Knoxville. He is a senior member of IEEE and IISE; member of ACM and AAAI. His email address is omitaomuoa@ornl.gov.

XUEPING LI is a Professor and Dan Doulet Faculty Fellow of Industrial and Systems Engineering and the Director of the Ideation Laboratory (iLab) and co-Director of the Health Innovation Technology and Simulation (HITS) Lab at the University of Tennessee - Knoxville. He holds a Ph.D. from Arizona State University. His research areas include complex system modeling, simulation, and optimization, with broad applications in supply chain logistics, healthcare, and energy systems. He is an IISE Fellow and a member of IEEE, ASEE, and INFORMS. His e-mail address is Xueping.Li@utk.edu. His website is https://xli.tennessee.edu/.